Received: 23 April 2022 | Revised: 9 October 2022 | Accepted: 13 October 2022

DOI: 10.1111/cas.15632

Cancer Science WILEY

ORIGINAL ARTICLE

BAIAP2L1 accelerates breast cancer progression and chemoresistance by activating AKT signaling through binding with ribosomal protein L3

Ning Deng[1] | Xiupeng Zhang[2] | Yong Zhang[3]

[1]Department of Breast Surgery, Cancer Hospital of China Medical University, Liaoning Cancer Hospital and Institute, Shenyang, China

[2]Department of Pathology, College of Basic Medical Sciences and First Affiliated Hospital, China Medical University, Shenyang, China

[3]Department of Pathology, Cancer Hospital of China Medical University, Liaoning Cancer Hospital and Institute, Shenyang, China

Correspondence
Yong Zhang, Department of Pathology, Cancer Hospital of China Medical University, Liaoning Cancer Hospital and Institute, No. 44 Xiaoheyan Road, Dadong District, Shenyang 110042, Liaoning, China.
Email: zhycmu@163.com

Funding information
Fundamental Research Funds for Central Universities, Grant/Award Number: LD202121

Abstract

BAI1-associated protein 2-like 1 (BAIAP2L1), also known as insulin receptor tyrosine kinase substrate, modulates the insulin network; however, its function in breast cancer has not been explored. Immunohistochemical analysis of 140 breast cancer specimens (77 triple-negative and 63 nontriple-negative cases) indicated that BAIAP2L1 expression was higher in breast cancer tissues (56/140, 40%) than in normal breast tissues (28.3%, 15/53; $p < 0.001$). BAIAP2L1 expression in breast cancer was correlated with triple-negative breast cancer ($p = 0.0013$), advanced TNM stage ($p = 0.001$), lymph node metastasis ($p = 0.001$), and poor patient prognosis ($p = 0.001$). BAIAP2L1 overexpression could accelerate breast cancer proliferation, invasion, and stemness in vivo and in vitro, possibly through the activation of AKT, Snail, and cyclin D1. Treatment with the AKT inhibitor LY294002 reduced the effects of BAIAP2L1 overexpression on breast cancer cells. BAIAP2L1 may bind to the AA202-288 of ribosomal protein L3 (RPL3) within its SRC homology 3 (SH3) domain, the loss of which may abolish the transduction of the AKT signaling pathway by promoting the degradation of PIK3CA. Moreover, BAIAP2L1 overexpression may induce chemotherapy resistance, with BAIAP2L1 expression being higher in patients with advanced Miller grades than those with lower grades. Our results indicated that BAIAP2L1 promotes breast cancer progression through the AKT signaling pathway by interacting with RPL3 through its SH3 domain.

KEYWORDS
AKT, BAIAP2L1, breast cancer, chemoresistance, PIK3CA, RPL3

Abbreviations: ALDH1, aldehyde dehydrogenase 1; BAIAP2L1, BAI1-associated protein 2-like 1; CAP1, cyclase-associated protein 1; CHX, cycloheximide; Co-IP, co-immunoprecipitation; CSC, cancer stem cell; DEG, differentially expressed gene; EMT, epithelial–mesenchymal transition; ER, estrogen receptor; FDR, false discovery rate; GO, Gene Ontology; GSEA, Gene Set Enrichment Analysis; HER2, human epidermal growth factor receptor-2; I-BAR, inverse BAR; IRKTS, insulin receptor tyrosine kinase substrate; LC-MS/MS, liquid chromatography–tandem mass spectrometry; MP, Miller–Payne; MS, mass spectrometry; PR, progesterone receptor; RPL3, ribosomal protein L3; sgRNA, single guide RNA; SH3, SRC homology 3; TCGA, The Cancer Genome Atlas; TNBC, triple-negative breast cancer.

1 | INTRODUCTION

Breast cancer is the most diagnosed cancer, with an estimated 2.3 million new cases per year.[1] Based on the expression of ER, PR, and HER2, breast cancer can be classified into luminal, HER2-overexpressing, and basal-like subtype.[2,3] Triple-negative breast cancer (ER^-, PR^-, and $HER2^-$ TNBC) dominated most diagnosed basal-like subtypes. In contrast to hormone therapy in luminal and targeted therapy in the HER2 subtypes, it has no effective clinical therapy treatment. Chemotherapy remains the first-line therapy for TNBC, with the consequence of increased resistance to treatment. Cancer stem cells are an expanded population during breast cancer progression and have been proven to induce chemotherapy resistance.[4–7] Therefore, eliminating CSCs is an outstanding issue that needs to be resolved.

BAI1-associated protein 2-like is also known as insulin receptor tyrosine kinase substrate (IRTKS). It consists of an I-BAR domain at the N-terminus, a central SH3 domain, and an F-actin binding domain at the C-terminus. BAIAP2L1 is highly expressed in ovarian cancer,[8] lung cancer,[9] gastric cancer,[10] and hepatocellular carcinoma.[11] Its expression promotes cancer progression and a malignant phenotype. However, its role in breast cancer and chemotherapy resistance has not been investigated.

In this study, we observed that BAIAP2L1 might accelerate breast cancer cell proliferation and invasion by activating the AKT signaling pathway by binding with RPL3 through its SH3 domain by high-throughput RNA sequencing and MS analyses.

2 | MATERIALS AND METHODS

2.1 | Patients and clinical specimens

The study protocol was approved by the Institutional Review Board of China Medical University. All participants provided written informed consent, and the study was carried out according to the Declaration of Helsinki principles. Primary tumor specimens were obtained from 140 patients with breast cancer, including 77 patients with TNBC and 63 patients with non-TNBC. All patients diagnosed with invasive ductal carcinoma underwent complete surgical resection at the Affiliated Cancer Hospital of China Medical University between 2001 and 2003. Complete follow-up data (from 2003 to 2014) were available for all the 140 patients. Patient survival was defined as the time from the day of surgery to the end of the follow-up period or the date of death due to recurrence or metastasis. None of the patients had received radiotherapy or chemotherapy before undergoing surgical resection, and all patients were treated with routine chemotherapy after surgery. An additional 256 patients, who received neoadjuvant chemotherapy treatment from 2010 to 2021, were included. Of these, 20 patients were diagnosed as luminal A subtype, 143 luminal B, 63 Her2 overexpressing, and 30 TNBC. One hundred and sixty-eight patients receive E (epirubicin) + C (cyclophosphamide) plans for four cycles followed by T (docetaxel) for four cycles and 62 received TEC plans for six cycles, 26 patients received TCbH plans (docetaxel + carboplatin + trastuzumab) for six cycles. One hundred and nineteen patients were classified as Miller–Payne (MP)[12] grade 1 and 2, and the other 137 patients were MP grade 3–5.

A total of 16 freshly isolated specimens, including both tumor tissue and the corresponding normal tissues, were stored at −70°C immediately after resection for subsequent protein extraction.

2.2 | Immunohistochemistry

Immunohistochemical analysis was undertaken as previously described.[13] Tissue sections were incubated with rabbit polyclonal Abs against BAIAP21L (1:50; Sigma), p-AKT at Ser473 (1: 100; Cell Signaling Technology). BAIAP2L1 and p-AKT staining intensities were scored as 0, 1, 2, and 3, corresponding to no signal, weak, moderate, or high signals, respectively. The percentage of stained cells was scored as 1, 1–25%; 2, 26–50%; 3, 51–75%; and 4, 76–100%. The staining intensity score and the percentage of stained cells score for each tumor sample were multiplied to give a final score from 0–12; tumors with a score of 4 or higher were considered to have strong expression, whereas those with a score of less than 4 were considered to have a negative or weak expression of BAIAP2L1 and p-AKT.

2.3 | Cell lines

MCF-7, SK-BR-3, MDA-MB-231, and MDA-MB-453 cell lines were obtained from Shanghai Cell Bank. All cells were cultured in RPMI-1640 medium (Invitrogen) containing 10% FCS (Invitrogen), 100 IU/mL penicillin, and 100 μg/mL streptomycin (Sigma-Aldrich). The cells were grown in sterile culture dishes at 37°C in a 5% CO_2 atmosphere and passaged every 2 days, using 0.25% trypsin (Invitrogen) for cell detachment. All cell lines were authenticated using short tandem repeat DNA profiling.

2.4 | Western blot analysis and immunoprecipitation

As described by Dong et al.[14] Detailed descriptions of Abs are found in Appendix S1.

2.5 | Immunofluorescent staining

Detailed descriptions are found in Appendix S1.

2.6 | Calculation of image colocation coefficient

Detailed descriptions are found in Appendix S1.

2.7 | Plasmid transfection and siRNA treatment

Plasmids pCMV6-ddk-myc and pCMV6-ddk-myc-BAIAP2L1 were purchased from Origene. RPL3- (sc-152,909) and NC-siRNA (sc-37,007) were purchased from Santa Cruz Biotechnology. Control and BAIAP2L1 sgRNA, BAIAP2L1-ΔI-BAR, BAIAP2L1-ΔSH3, BAIAP2L1-ΔF actin-binding, RPL3-FL, RPL3-Δ1-43, and RPL3-Δ203-287 splicing mutant plasmids were purchased from GenePharma Co. Ltd. BAIAP2L1-sgRNA (CGCCAAGGTAGCCCTGAACGTGG) and its control sgRNA (GCACTACCAGAGCTAACTTCA) were made using a lentiviral vector (pLenti-U6-spgRNAv2.0-CMV-Puro-P2A-3xFLAG-spCas9-WPRE; GenePharma). Transfection was carried out using Lipofectamine 3000 reagent (Invitrogen) according to the manufacturer's instructions. Puromycin (ST551; Beyotime) was used to screen stably transfected cells.

2.8 | Cell proliferation and colony formation assay

Detailed descriptions are found in Appendix S1.

2.9 | Flow cytometry for cell cycle and apoptosis analysis

Detailed descriptions are found in Appendix S1.

2.10 | Matrigel invasion assay

Detailed descriptions are found in Appendix S1.

2.11 | Sphere formation assay

Breast cancer cells stably overexpressing or knocking out BAIAP2L1 were resuspended in RPMI-1640 supplemented with B27 (20 ng/mL), fibroblast growth factor-basic, and 20 ng/mL epidermal growth factor (Thermo Fisher Scientific). The cells were plated in a 96-well, ultra-low attachment microplate (Corning) at a density of 1000 cells/well. After 14 days, the spheres (defined as >70 cells/spheroid) were observed using an inverted TE300 microscope (Nikon Co. Ltd).

2.12 | RNA sequencing

Total RNA was extracted from the control and BAIAP2L1 KO MDA-MB-231 cells using TRIzol reagent (Takara), according to the manufacturer's instructions. RNA purity was tested using a NanoPhotometer spectrophotometer (Implen). cDNA libraries were constructed from 1 μg total RNA using a PCR-cDNA Sequencing Kit (SQK-PCS109; Nanopore Technologies), according to the manufacturer's protocol. Genes with an FDR less than 0.05 and fold change of 1.0 or more, found by DESeq (https://bioconductor.org/packages/DESeq2/), were designated as "differentially expressed."

2.13 | Functional enrichment analyses

Database for Annotation, Visualization, and Integrated Discovery (DAVID) (https://david.ncifcrf.gov/summary.jsp), an online tool for gene functional enrichment, was used for GO analysis (cellular component, molecular function, and biological process) and Kyoto Encyclopedia of Genes and Genomes pathway analysis of the 597 DEGs shared between high and low expression of the BAIAP2L1 group. The results were visualized using the ggplot2 R package. Statistical significance was set at $p < 0.05$. Gene Set Enrichment Analysis was adopted to identify the signaling pathways involved in the elevated BAIAP2L1-related gene signature in breast cancer patients. Statistical significance was set at $p < 0.05$. The pathways used for GSEA were obtained from the Molecular Signatures Database (MSigDB) (http://software.broadinstitute.org/gsea/msigdb).

2.14 | Liquid chromatography–MS/MS analysis

Proteins in the gel pieces from co-immunoprecipitation (Co-IP) in BAIAP2L1-overexpressing SK-BR-3 cells were analyzed by nano-LC-MS/MS analysis performed on a Q Exactive mass spectrometer (Thermo Scientific) coupled to an Easy nLC system (Thermo Fisher Scientific). Raw MS/MS data were converted into an MGF format using Proteome Discoverer 1.4 (Thermo Fisher Scientific). Peptide identification was performed using Mascot software (Version 2.3.01, Matrix Science, UK) using the UniProt database search algorithm and the integrated FDR analysis function. The data were searched against a protein sequence database, downloaded from 2021_uni_mus (128,510 sequences; 62,817,431 residues). The MS/MS spectra were searched against a decoy database to estimate the false discovery rate (FDR < 0.05) for peptide identification.

2.15 | Transplantation of tumor cells into nude mice

The animals used in this study were treated according to the NIH Guide for the Care and Use of Laboratory Animals (NIH Publications No. 8023, revised 1978). Four-week-old female BALB/c nude mice were purchased from Slac and maintained in a laminar-flow cabinet, under specific pathogen-free conditions, for 2 weeks before use. Each mouse was then inoculated subcutaneously with 5×10^6 of BAIAP2L1 KO (referred as BAIAP2L1$^{-/-}$) or control tumor cells in 0.2 ml sterile PBS. To measure the effect on metastatic abilities, 2×10^6 BAIAP2L1$^{-/-}$ or control tumor cells in 0.2 ml sterile PBS were injected intravenously (tail vein). Six or 10 weeks after inoculation, the mice were killed and examined for tumor growth and dissemination. The tumors, hearts, livers, lungs, and kidneys were dissected, fixed in 4% formaldehyde

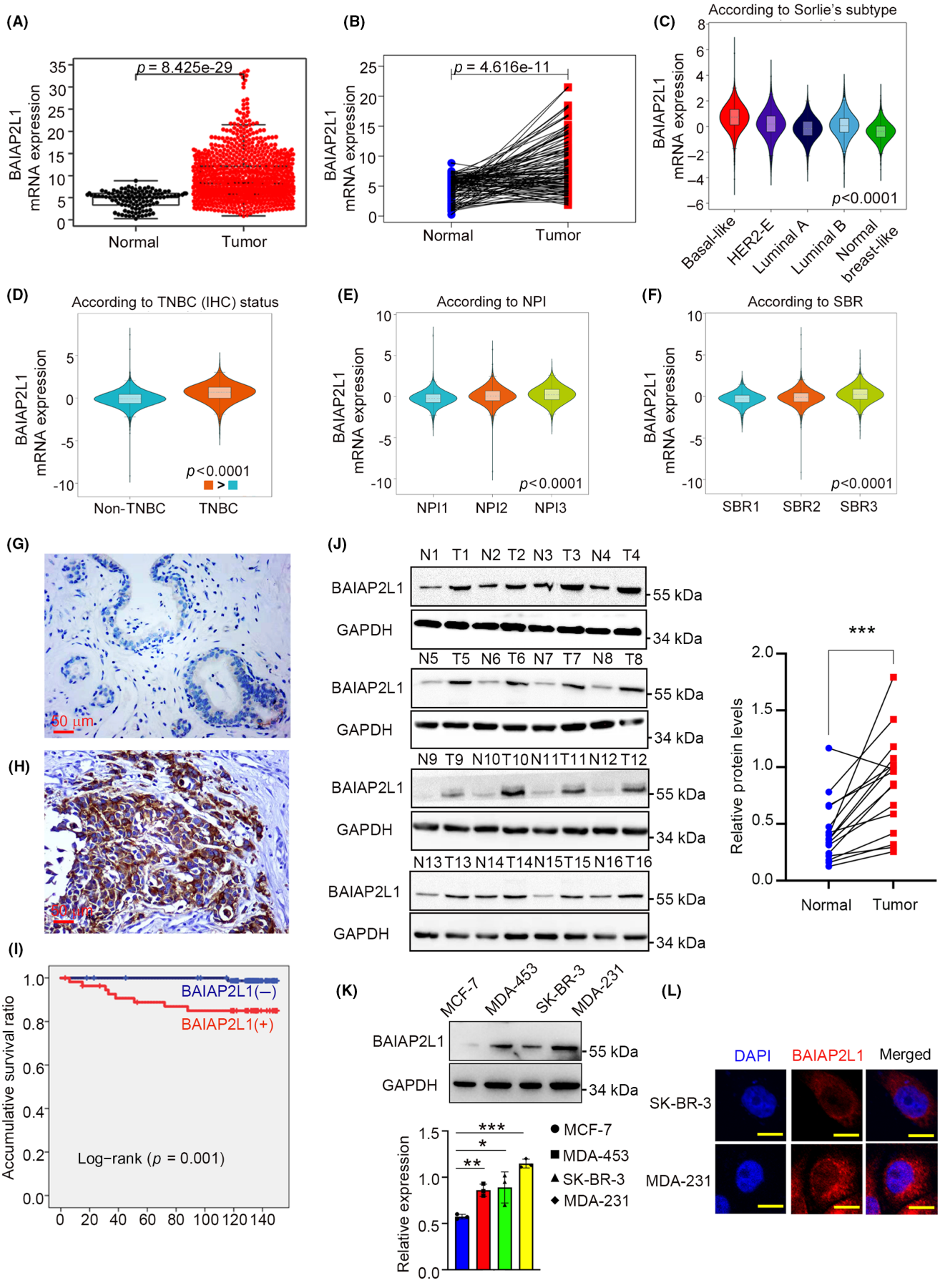
(A)
p = 8.425e-29
BAIAP2L1 mRNA expression
Normal
Tumor
(B)
p = 4.616e-11
BAIAP2L1 mRNA expression
Normal
Tumor
(C)
According to Sorlie's subtype
BAIAP2L1 mRNA expression
p<0.0001
Basal-like
HER2-E
Luminal A
Luminal B
Normal breast-like
(D)
According to TNBC (IHC) status
BAIAP2L1 mRNA expression
p<0.0001
Non-TNBC
TNBC
(E)
According to NPI
BAIAP2L1 mRNA expression
p<0.0001
NPI1
NPI2
NPI3
(F)
According to SBR
BAIAP2L1 mRNA expression
p<0.0001
SBR1
SBR2
SBR3
(G)
50 μm
(H)
50 μm
(I)
Accumulative survival ratio
BAIAP2L1(−)
BAIAP2L1(+)
Log−rank (p = 0.001)
(J)
N1 T1 N2 T2 N3 T3 N4 T4
BAIAP2L1
55 kDa
GAPDH
34 kDa
N5 T5 N6 T6 N7 T7 N8 T8
BAIAP2L1
55 kDa
GAPDH
34 kDa
N9 T9 N10 T10 N11 T11 N12 T12
BAIAP2L1
55 kDa
GAPDH
34 kDa
N13 T13 N14 T14 N15 T15 N16 T16
BAIAP2L1
55 kDa
GAPDH
34 kDa
***
Relative protein levels
Normal
Tumor
(K)
MCF-7
MDA-453
SK-BR-3
MDA-231
BAIAP2L1
55 kDa
GAPDH
34 kDa
***
*
**
Relative expression
MCF-7
MDA-453
SK-BR-3
MDA-231
(L)
DAPI
BAIAP2L1
Merged
SK-BR-3
MDA-231

FIGURE 1 BAIAP2L1 was highly expressed in the cytoplasm and correlated with poor prognosis. (A, B) BAIAP2L1 mRNA levels between noncancerous and cancerous tissues identified using The Cancer Genome Atlas database. (C) Comparison of BAIAP2L1 mRNA expression among different subtypes of breast cancer. (D) Comparison of BAIAP2L1 mRNA expression between triple-negative breast cancer (TNBC) and non-TNBC. (E) Comparison of BAIAP2L1 mRNA expression according to the Nottingham Prognostic Index (NPI) scores. (F) Comparison of BAIAP2L1 mRNA expression levels according to Scarff–Bloom–Richardson (SBR) grades. (G, H) Representative image of immunohistochemistry (IHC) staining of BAIAP2L1 in patients with breast cancer. Scale bar, 50 μm. (I) Correlation between BAIAP2L1 protein levels and overall survival of patients with breast cancer. (J) BAIAP2L1 protein in 16 freshly isolated samples from patients with breast cancer analyzed by western blotting. N, normal tissue; T, tumor tissue. (K, L) BAIAP2L1 protein levels and subcellular localization detected by western blotting and immunofluorescence assays, respectively. Quantification data are expressed as mean ± SD of three independent experiments. *$p < 0.05$, **, $p < 0.01$, ***$p < 0.001$, *t* test

(Sigma), and embedded in paraffin. Serial 6 μm-thick sections were cut, stained with H&E, and examined by microscopy.

2.16 | Statistical analysis

All data were analyzed using SPSS 22.0 (SPSS, Inc.). The χ^2-test was used to test the correlation between BAIAP2L1 expression and clinicopathologic factors. All clinicopathologic parameters were included in the Cox regression model and tested by univariate and multivariate analyses using the enter method. Student's t-test was used to analyze differences between groups. The one-way ANOVA test was used to compare multiple group. A *p* value less than 0.05 (two-sided) was considered statistically significant.

3 | RESULTS

3.1 | BAIAP2L1 highly expressed in breast cancer and correlated with malignant phenotype and poor prognosis

We first analyzed BAIAP2L1 mRNA expression in normal and cancerous samples using the TCGA database. This showed that BAIAP2L1 mRNA was highly expressed in breast cancer specimens compared to paired normal tissues (Figure 1A,B). BAIAP2L1 was relatively highly expressed in basal-like breast cancer compared to other cancer types (Figure 1C). BAIAP2L1 mRNA expression was significantly higher in TNBC than in non-TNBC (Figure 1D). Moreover, increased BAIAP2L1 expression was positively correlated with a poor Nottingham Prognostic Index and higher Scarff–Bloom–Richardson[15] grades (Figure 1E,F).

Next, we explored the protein expression and subcellular localization in breast cancer specimens and cell lines. Immunohistochemistry assays indicated that BAIAP2L1 was highly expressed in the cytoplasm of breast cancer samples (56/140, 40%) compared to noncancerous tissues (5/61, 8.2%, $p < 0.001$; Figure 1G,H). Immunofluorescence staining also revealed that the BAIAP2L1 protein was localized in the cytoplasm of breast cancer cells (Figure S1A). BAIAP2L1 expression positively correlated with advanced TNM stage ($p = 0.001$), lymph node metastasis ($p = 0.001$), and TNBC ($p = 0.013$), but not with age ($p = 0.864$; Table 1). Kaplan–Meier analysis indicated that the survival of patients with BAIAP2L1 overexpression (133.779 ± 5.442 months) was significantly shorter than those who were BAIAP2L1-negative (149.564 ± 0.433 months, $p = 0.001$; Figure 1I). To further explore correlation between BAIAP2L1 expression and different subtype of breast cancer, TCGA data revealed that BAIAP2L1 expression significantly correlated with poor prognosis in TNBC ($p = 0.0354$) rather than the other subtypes of breast cancer (Figure S1B). However, Cox univariate

TABLE 1 Correlation of BAIAP2L1 overexpression with clinicopathologic features in 140 cases breast cancer

Clinicopathologic factors	*n*	Positive	Negative	χ^2-test	*p* value
Age (years)					
<52	74	29	45	0.043	0.864
≥52	66	27	39		
TNM classification					
I + II	95	29	66	11.053	0.001
III	45	27	18		
Lymph node metastasis					
Positive	55	31	24	10.107	0.001
Negative	85	60	25		
Triple-negative(ER, PR, HER2)					
Positive	77	38	39	6.234	0.013
Negative	63	18	45		

ER, estrogen receptor; HER2, human epidermal growth factor receptor-2; PR, progesterone receptor.

TABLE 2 Summary of Cox univariate and multivariate regression analyses of the association between clinicopathologic features and overall survival in 146 cases of breast cancer

Clinicopathologic feature	Regression coefficient	Wald χ^2-test	*p* value	Risk ratio	95% confidence interval	
					Lower	Upper
Univariate analysis						
Age	−0.586	0.688	0.407	0.556	0.139	2.224
TNM classification	2.129	7.048	0.008	8.410	1.746	40.505
Lymph node metastasis	2.652	6.247	0.012	14.179	1.772	113.418
Triple-negative	0.494	0.488	0.485	1.639	0.410	6.552
BAIAP2L1 expression	2.592	5.968	0.015	13.351	1.669	106.781
Multivariate analysis						
BAIAP2L1 expression	1.971	3.207	0.073	7.719	0.830	62.074

and multivariate analyses revealed that cytosolic BAIAP2L1 overexpression was not an independent prognostic factor in breast cancer ($p = 0.073$; Table 2). The western blot analysis also suggested that the BAIAP2L1 protein levels in neoplastic tissues were significantly higher than those in paired normal breast tissues ($p = 0.0003$; Figure 1J). BAIAP2L1 expression was also detected in four breast cancer cell lines; this was higher in MDA-MB-231 cells than in the other cell lines (MCF-7, SK-BR-3, and MDA-MB-453; Figure 1K). Immunofluorescence assays confirmed that BAIAP2L1 was localized in the cytoplasm in both breast cancer cell lines (Figure 1L). Overall, our results indicated that BAIAP2L1 was highly expressed in the cytoplasm of breast cancer specimens and cell lines and was correlated with breast cancer progression and poor prognosis.

3.2 | BAIAP2L1 promoted breast cancer cell proliferation in vitro and in vivo

BAIAP2L1 was overexpressed by transfection with a BAIAP2L1 plasmid in SK-BR-3 and MCF-7 cells or depleted using sgRNA in MDA-MB-231 and MDA-MB-453 cells (Figures 2A and S2A,B). First, we undertook GSEA and found that DEGs enriched on increased BAIAP2L1 expression were positively correlated with the cell cycle (Figure 2B). The MTT and colony formation assays suggested that proliferation was enhanced by BAIAP2L1 overexpression or suppressed by its silencing in SK-BR-3 and MCF-7 or MDA-MB-231 and MDA-MB-453 cells (Figures 2C,D and S2C,D). Flow cytometry assays revealed that G_1/S transition was enhanced when BAIAP2L1 was overexpressed in SK-BR-3 and MCF-7 cells and abrogated when BAIAP2L1 was silenced in MDA-MB-231 and MDA-MB-453 cells (Figures 2E and S2E). Western blotting results showed that the expression of cyclin D1 was upregulated when BAIAP2L1 was overexpressed in MCF-7, SK-BR-3, and MDA-MB-231 cells or downregulated on inhibiting BAIAP2L1 in SK-BR-3, MDA-MB-231, and MDA-MB-453 cells (Figures 2F and S2F). Next, we tested in vivo the effect on proliferation induced by modulation of BAIAP2L1. This indicated that the volume of xenografts was significantly abrogated by depleting BAIAP2L1 using sgRNA in MDA-MB-231 cells (Figure 2G,H).

3.3 | BAIAP2L1 increased invasive and stem cell abilities by modulating EMT in vitro and in vivo

We undertook a Transwell assay to explore the effects of modulating BAIAP2L1 on invasion. Our results suggested that the invasion of breast cancer cells was accelerated by BAIAP2L1 upregulation in SK-BR-3 and MCF-7 cells or abolished by knocking out BAIAP2L1 by sgRNA in MDA-MB-231 and MDA-MB-453 cells (Figures 3A and S3A). Subsequent western blotting assays showed that Snail, which is crucial for the induction of EMT,[16,17] was increased after BAIAP2L1 overexpression in SK-BR-3, MCF-7, and MDA-MB-231 cells and decreased by silencing BAIAP2L1 in SK-BR-3, MDA-MB-231, and MDA-MB-453 cells. In contrast, E-cadherin was abrogated by overexpression of BAIAP2L1 and augmented by silencing BAIAP2L1; however, Slug, N-cadherin, and Vimentin were not altered in all the cells detected (Figures 3B and S3B). Previous studies have reported that the EMT process might enhance clonogenic abilities by increasing the cancer stem cell ratios.[5–7] A sphere

FIGURE 2 BAIAP2L1 (BAI) accelerated breast cancer proliferation both in vitro and in vivo. (A) Up- or downregulation of BAIAP2L1 expression confirmed by western blot analysis in SK-BR-3 cells and MDA-MB-231 cells. (B) Gene Set Enrichment Analysis, to explore the signaling pathway that was positively correlated with high BAIAP2L1 expression in breast cancer. FDR, false discovery rate; KEGG, Kyoto Encyclopedia of Genes and Genomes; NES, normalized enrichment score. (C) MTT, (D) colony formation, and (E) cell cycle assays were carried out to detect the effect on the proliferation of SK-BR-3 and MDA-MB-231 cells following BAIAP2L1 overexpression or depletion. Dip, diploid. (F) Western blot analysis was used to identify the levels of the cell cycle-related proteins after BAIAP2L1 overexpression or knockout. (G) Representative examples of explanted tumors in the MDA-MD-231-BAIAP2L1 and -NC study group. (H) Quantification data of the explanted tumors expressed as average ± SD of three independent experiments. $^*p < 0.05$, $^{**}p < 0.01$, *t*-test, two-sided. sgNC, sgRNA negative control

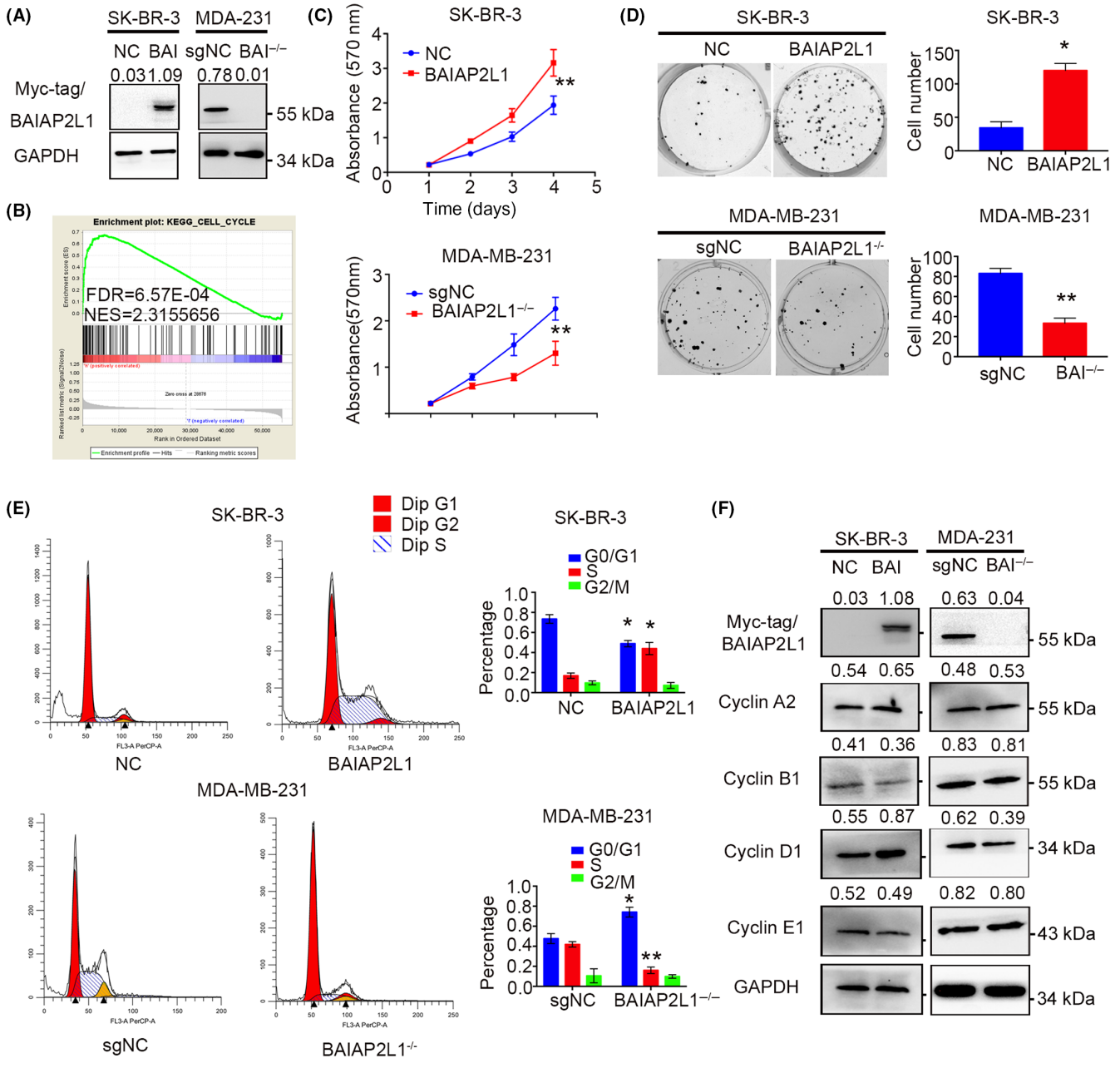
(A)
SK-BR-3
MDA-231
NC BAI sgNC BAI−/−
0.03 1.09 0.78 0.01
Myc-tag/
BAIAP2L1
GAPDH
55 kDa
34 kDa
(B)
Enrichment plot: KEGG_CELL_CYCLE
FDR=6.57E-04
NES=2.3155656
(C)
SK-BR-3
NC
BAIAP2L1
Absorbance (570 nm)
Time (days)
MDA-MB-231
sgNC
BAIAP2L1−/−
Absorbance(570nm)
(D)
SK-BR-3
NC
BAIAP2L1
Cell number
MDA-MB-231
sgNC
BAIAP2L1-/-
Cell number
(E)
Dip G1
Dip G2
Dip S
SK-BR-3
NC
BAIAP2L1
G0/G1
S
G2/M
Percentage
MDA-MB-231
sgNC
BAIAP2L1−/−
(F)
SK-BR-3
MDA-231
NC BAI sgNC BAI−/−
0.03 1.08 0.63 0.04
Myc-tag/
BAIAP2L1
55 kDa
0.54 0.65 0.48 0.53
Cyclin A2
55 kDa
0.41 0.36 0.83 0.81
Cyclin B1
55 kDa
0.55 0.87 0.62 0.39
Cyclin D1
34 kDa
0.52 0.49 0.82 0.80
Cyclin E1
43 kDa
GAPDH
34 kDa
(G)
sgNC
BAIAP2L1−/−
(H)
sgNC
BAIAP2L1−/−
Tumor volume (cm3)

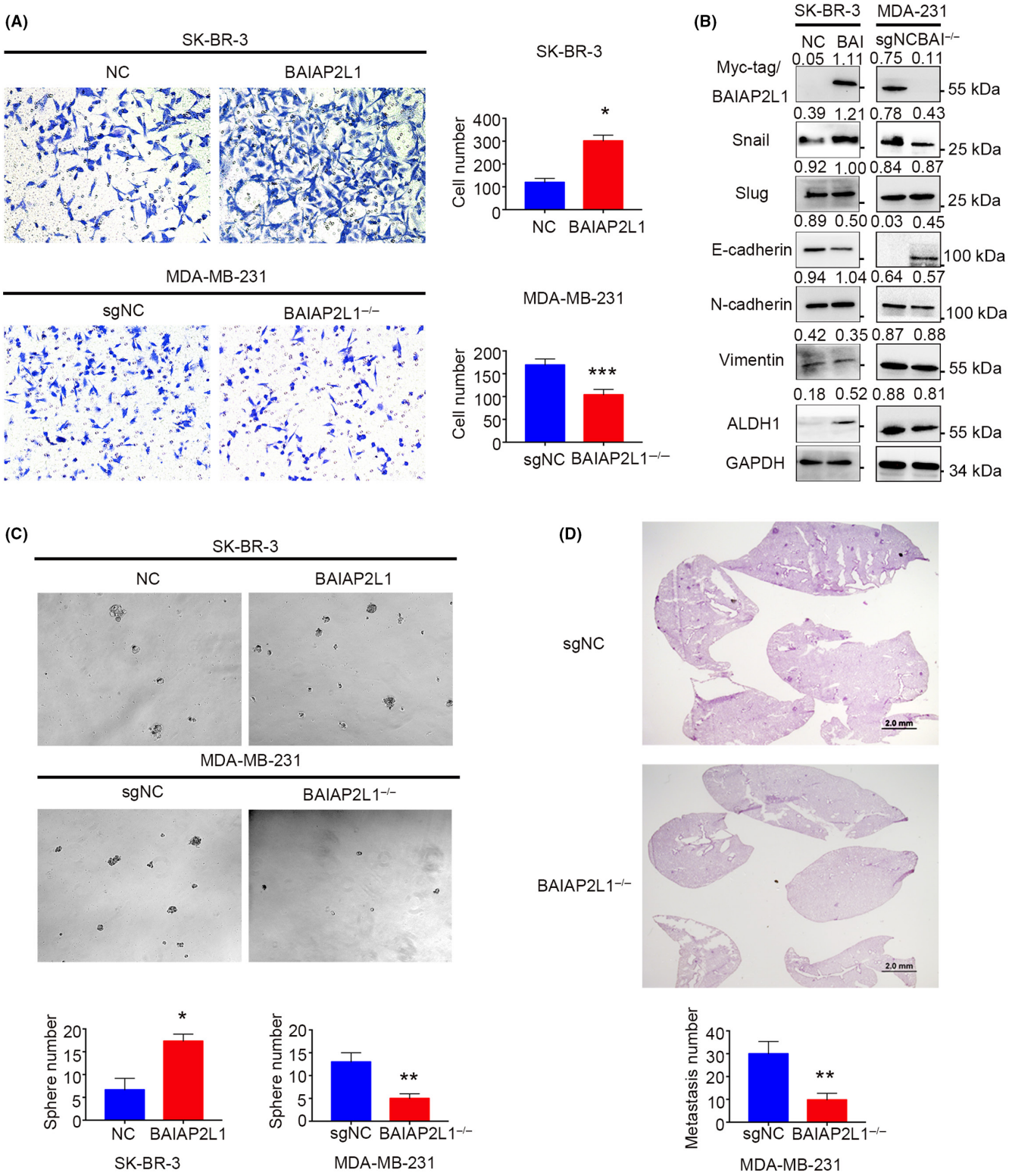

FIGURE 3 BAIAP2L1 (BAI) promoted invasion and cancer stem cell abilities by inducing epithelial–mesenchymal transition (EMT). (A) Transwell assay revealed the effect on invasive abilities following overexpression or silencing of BAIAP2L1 in SK-BR-3 or MDA-MB-231 cells. (B) Western blot analysis of EMT-related and cancer stem cell protein expression profiles. (C) Sphere formation assays were used to detect changes after overexpressing or inhibiting BAIAP2L1 in SK-BR-3 or MDA-MB-231 cells. (D) Representative examples of lung metastasis in the MDA-MD-231-BAIAP2L1 and MDA-MB-231-NC study groups, metastasized colonies were quantified by the Student's t test. Quantification data are expressed as average ± SD of three independent experiments. $^{*}p < 0.05$, $^{**}p < 0.01$, $^{***}p < 0.001$, *t*-test, two-sided. ALDH1, aldehyde dehydrogenase 1; NC, Negative control; sgNC, sgRNA negative control

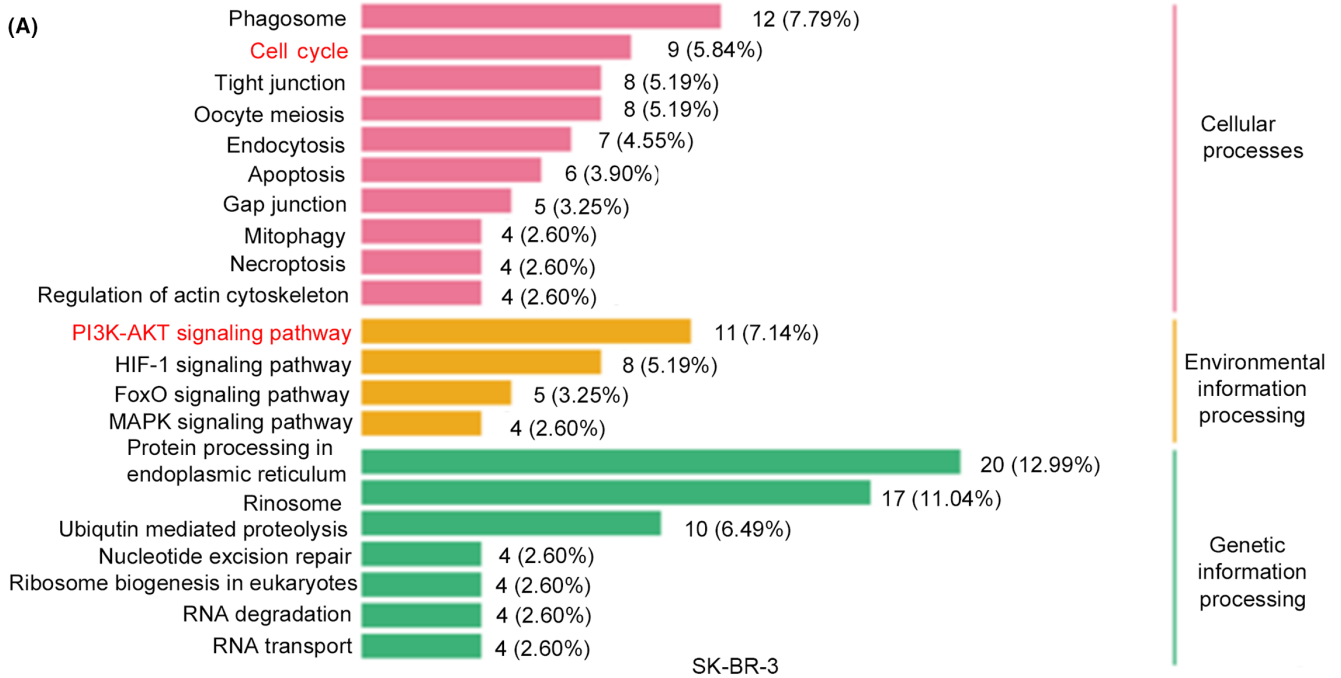
(A)
Phagosome 12 (7.79%)
Cell cycle 9 (5.84%)
Tight junction 8 (5.19%)
Oocyte meiosis 8 (5.19%)
Endocytosis 7 (4.55%)
Apoptosis 6 (3.90%)
Gap junction 5 (3.25%)
Mitophagy 4 (2.60%)
Necroptosis 4 (2.60%)
Regulation of actin cytoskeleton 4 (2.60%)
PI3K-AKT signaling pathway 11 (7.14%)
HIF-1 signaling pathway 8 (5.19%)
FoxO signaling pathway 5 (3.25%)
MAPK signaling pathway 4 (2.60%)
Protein processing in endoplasmic reticulum 20 (12.99%)
Rinosome 17 (11.04%)
Ubiqutin mediated proteolysis 10 (6.49%)
Nucleotide excision repair 4 (2.60%)
Ribosome biogenesis in eukaryotes 4 (2.60%)
RNA degradation 4 (2.60%)
RNA transport 4 (2.60%)
Cellular processes
Environmental information processing
Genetic information processing

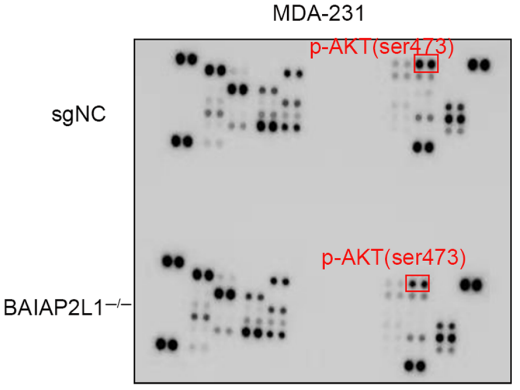
(B)
MDA-231
p-AKT(ser473)
sgNC
p-AKT(ser473)
BAIAP2L1−/−

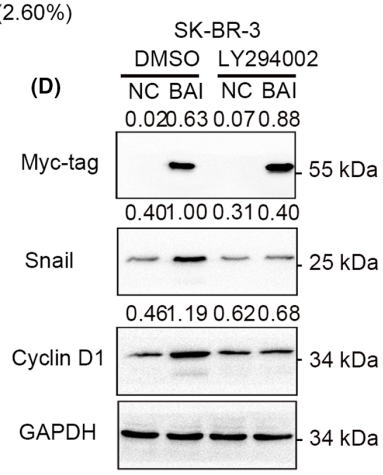
(D)
SK-BR-3
DMSO LY294002
NC BAI NC BAI
0.02 0.63 0.07 0.88
Myc-tag
55 kDa
0.40 1.00 0.31 0.40
Snail
25 kDa
0.46 1.19 0.62 0.68
Cyclin D1
34 kDa
GAPDH
34 kDa

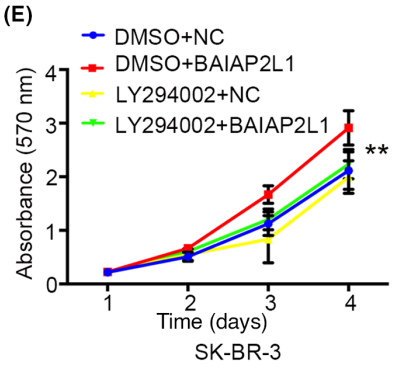
(E)
DMSO+NC
DMSO+BAIAP2L1
LY294002+NC
LY294002+BAIAP2L1
Absorbance (570 nm)
Time (days)
**
SK-BR-3

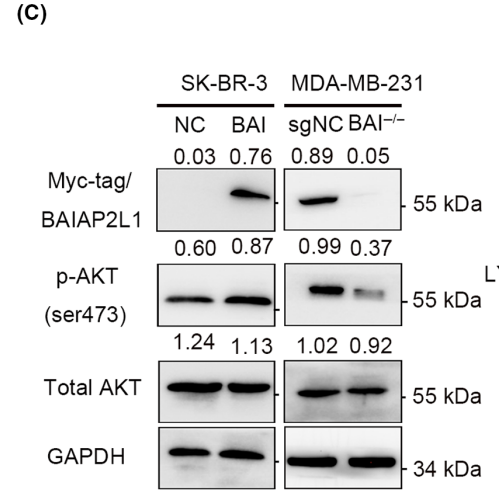
(C)
SK-BR-3 MDA-MB-231
NC BAI sgNC BAI−/−
0.03 0.76 0.89 0.05
Myc-tag/ BAIAP2L1
55 kDa
0.60 0.87 0.99 0.37
p-AKT (ser473)
55 kDa
1.24 1.13 1.02 0.92
Total AKT
55 kDa
GAPDH
34 kDa

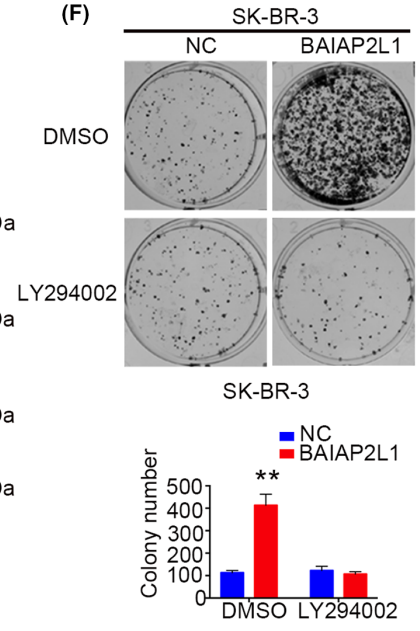
(F)
SK-BR-3
NC BAIAP2L1
DMSO
LY294002
SK-BR-3
NC
BAIAP2L1
Colony number
**
DMSO LY294002

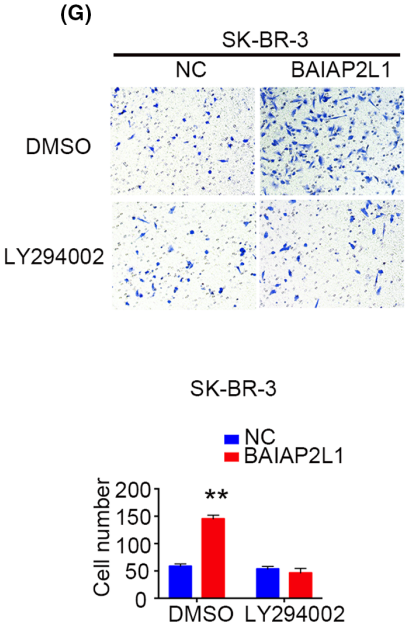
(G)
SK-BR-3
NC BAIAP2L1
DMSO
LY294002
SK-BR-3
NC
BAIAP2L1
Cell number
**
DMSO LY294002

FIGURE 4 BAIAP2L1 (BAI) enhanced breast cancer proliferation and invasion by activating the AKT signaling pathway. (A) Gene Ontology analysis exploring the signaling pathways positively correlated with high BAIAP2L1 expression in breast cancer. (B) Phospho-kinase Array Kit was used to screen the key signaling pathway involved in BAIAP2L1 depletion. Western blot analysis confirmed the (C) expression of phosphorylated AKT (p-AKT) in Ser473 and (D) expression of Snail and cyclin D1 after overexpressing BAIAP2L1, with or without AKT specific inhibitor LY294002. (E) MTT, (F) colony formation assay, and (G) Transwell assays were also used to investigate the effects on proliferation and invasion. Colony numbers were quantified by Student's *t*-test. Quantification data are expressed as average ± SD of three independent experiments. $^{**}p < 0.01$, *t*-test, two-sided

formation assay was undertaken to identify alterations in clonogenic abilities, which indicated that the number of spheres was increased with BAIAP2L1 overexpression in MCF-7 and SK-BR-3 cells and decreased on depleting BAIAP2L1 in MDA-MB-231 and MDA-MB-453 cells (Figures 3C and S3C). The cancer stem cell marker ALDH1 was accordingly upregulated on overexpression or downregulated on depletion of BAIAP2L1 (Figures 3B and S3B). Invasive abilities were also investigated by tail vein injection after knocking out BAIAP2L1 in MDA-MB-231 cells in vivo, indicating that lung metastasis foci were significantly reduced (Figure 3D).

3.4 | BAIAP2L1 promoted breast cancer progression by activating AKT signaling pathway

RNA sequencing assays were carried out to assess DEGs after BAIAP2L1 silencing. The analysis revealed that 109 genes were downregulated and 190 were upregulated, with a fold change greater than one, following BAIAP2L1 deletion in MDA-MB-231 cells (PRJNA880752, https://www.ncbi.nlm.nih.gov/bioproject/PRJNA880752/; Table S1). Gene Ontology analysis found that DEGs could be enriched for the cell cycle, which was similar to the results in the GSEA and PI3K-AKT signaling pathways (Figure 4A). The phospho-kinase array kit was used to screen the key signaling pathway involved in BAIAP2L1 expression; we found that phosphorylation of AKT at Ser473 was significantly reduced after knocking out BAIAP2L1 by sgRNA in MDA-MB-231 cells (Figure 4B). Subsequent western blotting results also showed that AKT phosphorylation was enhanced during BAIAP2L1 overexpression in MCF-7 and SK-BR-3 cells and abolished after its knockout in MDA-MB-231 and MDA-MB-453 cells (Figures 4C and S4A). This confirmed the RNA sequencing data. Next, we showed that treatment with PI3K-AKT pathway-specific inhibitor LY294002 to BAIAP2L1-overexpressing SK-BR-3 cells prevented the upregulation of Snail and cyclin D1 (Figure 4D), as well as the proliferation, apoptosis, and invasion of breast cancer cells (Figures 4E–G and S4B).

3.5 | BAIAP2L1 facilitated phosphorylation of AKT by stabilizing PIK3CA by interacting with RPL3 through the SH3 domain

To investigate how BAIAP2L1 modulates the AKT signaling pathway, we undertook protein interaction MS analysis in MDA-MB-231 cells to identify the underlying binding partner. The results revealed 404 latent binding partners (Table S2), from which we chose CAP1 and RPL3 for further study as they reportedly modulate breast cancer progression and the PI3K-AKT signaling pathway.[18–21] A Co-IP assay was used to evaluate the interaction between BAIAP2L1 and its potential binding partners. The endogenous and exogenous IP assay revealed that BAIAP2L1 might interact with RPL3 in MDA-MB-231 and SK-BR-3 cells (Figure 5A,B). Immunofluorescence assays also suggested that endogenous BAIAP2L1 colocalized with RPL3 in the cytoplasm of MDA-MB-231 cells ($r = 0.7754$; Figure 5C). To examine whether BAIAP2L1-promoted breast cancer progression was dependent on RPL3, we overexpressed BAIAP2L1 together with RPL3 siRNA and relative control in SK-BR-3 cells. Subsequent western blotting results indicated that elevated phosphorylation of AKT was counteracted by inhibition of RPL3 (Figure 5D). Enhanced proliferation and invasion induced by overexpression of BAIAP2L1 were also prevented by silencing RPL3 (Figure 5E,F). We should next map the specific domains responsible for the interaction between BAIAP2L1 and RPL3.

We constructed a series of splicing mutants of BAIAP2L1 or RPL3, referred to as BAI-FL, BAI-ΔI-BAR, BAI-ΔSH3, and BAI-ΔF-actin binding or RPL3-FL, RPL3-Mut1, and RPL3-Mut2 (Figure 5G). A subsequent Co-IP assay was carried out to identify the binding site, which showed that BAIAP2L1 might interact with RPL3 through the SH3 domain of BAIAP2L1[22] and AA202-288 of RPL3 (Figure 5H,I). BAI-FL, BAI-ΔSH3, and the control were transfected into SK-BR-3 cells. Western blot analysis indicated that the increased phosphorylation of AKT, Snail, and cyclin D1 by BAIAP2L1-FL overexpression was abrogated by the deletion of the BAIAP2L1 SH3 domain (Figure 6A). Proliferation and invasion were also decreased by overexpressing BAI-ΔSH3 compared to that by BAI-FL (Figure 6B–D).

To further explore how BAIAP2L1-RPL3 interaction activates the PI3K-AKT signaling pathway, we first undertook GSEA for RPL3 in breast cancer, it revealed DEGs enriched in RPL3 higher expression was positively correlated with ribosome and ubiquitin mediated proteolysis (Figure 6E). Our RNA sequencing data also revealed that DEGs within BAIAP2L1 KO MDA-MB-231 cells were also enriched in both processes, which indicated BAIAP2L1 might collaborate with RPL3 on modulating that. Previous studies had reported that PIK3CA, a key modulator of the PI3K-AKT signaling pathway, was controlled by ubiquitination.[23–25] A Co-IP assay was carried out and revealed that BAIAP2L1, RPL3, and PIK3CA could form a ternary complex (Figure 6F). Moreover, PIK3CA was stabilized by BAIAP2L1 KO following the addition of CHX to block the de novo protein synthesis (Figure 6G). Expression of PIK3CA as well as phosphorylation of AKT were also depressed by overexpressing RPL3-Mut2 (Δ AA202-288) compared with RPL3-FL in SK-BR-3 cells (Figure 6H). Overall, BAIAP2L1 could activate PI3K-AKT signaling by stabilizing PI3KCA dependent on binding with RPL3.

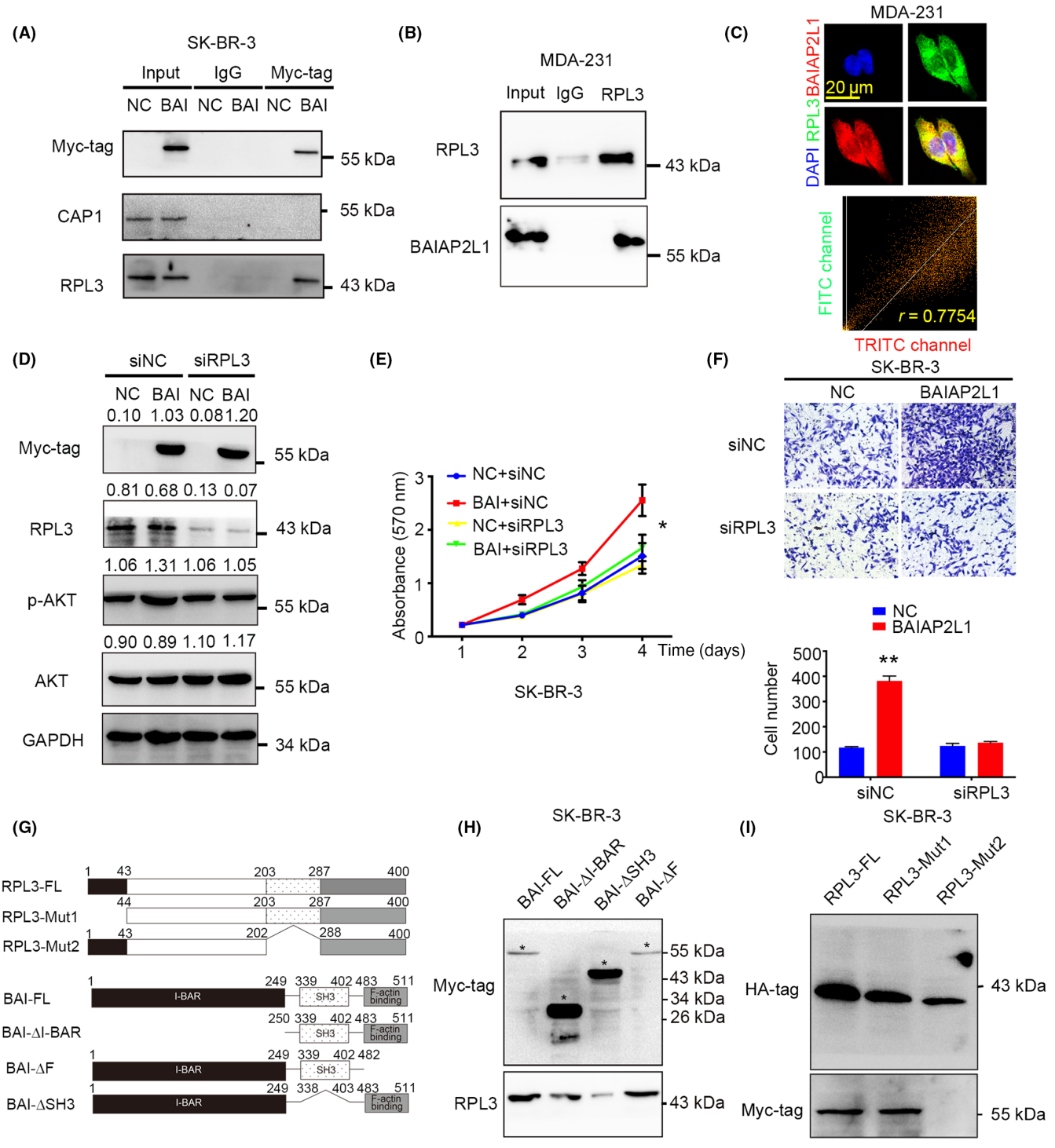

FIGURE 5 BAIAP2L1 (BAI) interacted with a.a. 202–208 of ribosomal protein L3 (RPL3) through its SRC homology 3 (SH3) domain. (A) Coimmunoprecipitation (Co-IP) assay was used to explore the interaction of BAIAP2L1 with RPL3 or cyclase-associated protein 1 (CAP1). (B) Endogenous Co-IP assay was used to explore the interaction between BAIAP2L1 and RPL3. (C) Immunofluorescence assay results show the subcellular colocalization of BAIAP2L1 and RPL3. (D) Western blot assay was assessed to checked the expression of AKT upon overexpressing BAIAP2L1 together with RPL3 knockdown in SK-BR-3 cells. (E) MTT and (F) Transwell assays were used to detect the effects on proliferation and invasion in SK-BR-3 cells. (G) Schematic diagram of myc-tagged BAIAP2L1 or HA-tagged encoding their full length and truncated proteins. (H, I) Co-IP assay revealed the domain responsible for the interaction between BAIAP2L1 and RPL3. Quantification data are expressed as average ± SD of three independent experiments. $^{*}p < 0.05$, $^{**}p < 0.01$, *t*-test, two-sided. FL, Full length; I-BAR, inverse BAR; Mut, mutant; NC, Negative control

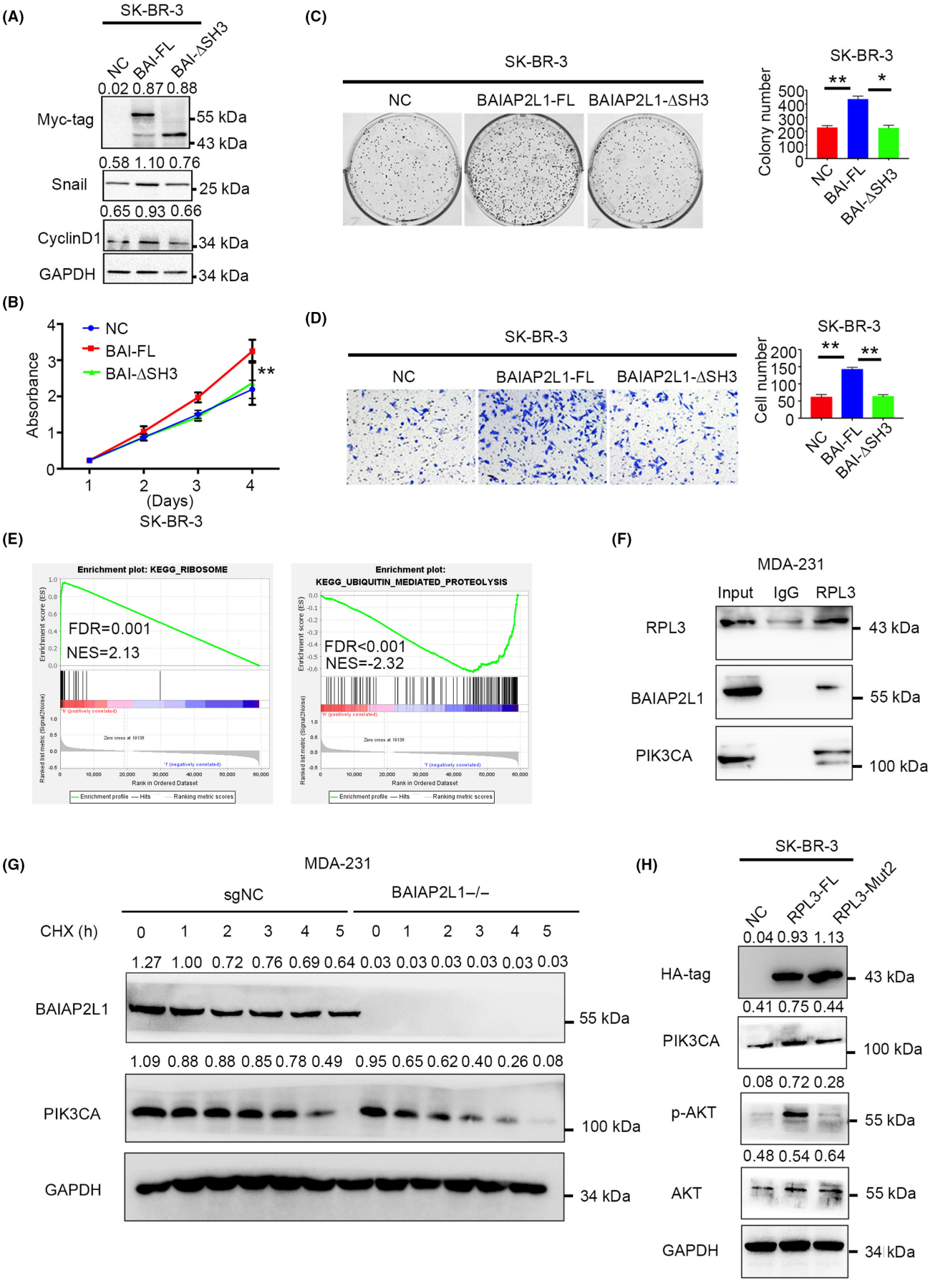

FIGURE 6 Legend on next page

FIGURE 6 BAIAP2L1 (BAI) activates the AKT signaling pathway by interacting with ribosomal protein L3 (RPL3) through its SRC homology 3 (SH3) domain. (A) Western blot analysis depicting the changes after transfection with BAIAP2L1-FL or BAIAP2L1-ΔSH3 plasmids. (B) MTT, (C) colony formation, and (D) Transwell assays were carried out to examine the effects on proliferation or invasion after overexpressing BAIAP2L1-FL or BAIAP2L1-ΔSH3 mutant. (E) Gene Set Enrichment Analysis was used to explore the signaling pathways positively correlated with high RPL3 expression in breast cancer. FDR, false discovery rate; KEGG, Kyoto Encyclopedia of Genes and Genomes; NES, normalized enrichment score. (F) RPL3 was immunoprecipitated from MDA-MB-231 cells and immunoblotted with indicated Abs. (G) After being treated with cycloheximide (CHX) at indicated time points, the expression of PIK3CA was evaluated by western blotting in MDA-MB-231 cells following BAIAP2L1 KO. (H) In SK-BR-3 cells overexpressing Flag-P130cas/Flag-P130-Mut2, immunoblotting was used to evaluate expression of phosphorylation of AKT and PIK3CA and GAPDH. Quantification data are expressed as average ± SD of three independent experiments. $^{*}p < 0.05$, $^{**}p < 0.01$, *t*-test, two-sided. NC, Negative control; sgNC, sgRNA negative control

3.6 | BAIAP2L1 promoted chemotherapy resistance in patients with breast cancer

Our study revealed that BAIAP2L1 might enhance the proliferation and invasion of breast cancer cells through the AKT signaling pathway by interacting with RPL3. Immunohistochemical staining was undertaken to confirm the relationship between BAIAP2L1 and p-AKT in human breast cancer specimens, which showed that positive or negative BAIAP2L1 expression significantly correlated with strong or dim expression of p-AKT ($p < 0.001$; Figure 7A and Table 3). Cancer stem cell expansion dominates resistance to chemotherapy.[26,27] The AKT signaling pathway is tightly connected to chemotherapy resistance.[28–30] To explore whether BAIAP2L1 induced chemotherapy resistance, we used docetaxel to induce chemotherapy resistance and measured IC_{50} values after treatment (Figure 7B). Western blot analysis indicated that BAIAP2L1 expression visibly increased in docetaxel-resistant MDA-MB-231 cells compared to that in the parental cells (Figure 7C). The breast cancer stem cell marker ALDH1 was also increased (Figure 7C). We also treated BAIAP2L1 stably-expressing cells with docetaxel, and subsequent colony formation assays suggested that BAIAP2L1 overexpression might counteract docetaxel-induced cell death (Figure 7D). Finally, immunohistochemical staining for BAIAP2L1 was assessed in breast cancer patients who received chemotherapy, and the MP grade was used to identify the treatment effect. BAIAP2L1 expression was significantly higher in MP grades 1 and 2 than in MP grades 3 and 4 ($p = 0.003$; Figure 7E). Our study revealed that BAIAP2L1 might induce chemotherapy resistance by promoting the AKT signaling pathway by binding to RPL3 (Figure 8).

4 | DISCUSSION

BAIAP2L1 is highly expressed in various malignant carcinomas, such as ovarian cancer,[8] lung cancer,[9] gastric cancer,[10] and hepatocellular carcinoma.[11] However, its expression pattern and biological function in breast cancer remain uncertain. Moreover, the correlation between BAIAP2L1 expression and chemotherapy effectiveness has not been discussed. In our study, both bioinformatics analyses and IHC staining indicated that BAIAP2L1 was relatively highly expressed in the cytoplasm of breast cancer tissues compared to noncancerous tissues, particularly in TNBC. Subsequent clinicopathologic factor analysis further revealed that BAIAP2L1 expression was positively correlated with advanced TNM stage, lymph node metastasis, and poor prognosis; however, BAIAP2L1 expression could not be evaluated as an independent risk factor for breast cancer progression.

The GSEA analysis, and our in vivo and in vitro studies, indicated that BAIAP2L1 might accelerate cell cycle phase transition and cancer stem cell abilities by modulating EMT, which has been proven to be a dominant process during tumor progression.[5–7] The RNA sequencing analysis helped identify DEGs after knocking out BAIAP2L1 by CRISPR-Cas9 technology. Subsequent GO analysis indicated that these DEGs might be involved in modulating the cell cycle, which was consistent with the results of GSEA. The Phospho-kinase Array Kit was used to screen the key signaling pathways responsible for the malignant phenotype of breast cancer induced by depleting BAIAP2L1. Phosphorylation of AKT at Ser 473 was abolished after knocking out BAIAP2L1, which was consistent with the results of the GO analysis. Interestingly, Wu et al. reported that BAIAP2L1 might activate the PI3K-AKT signaling pathway.[22] Our results indicate that BAIAP2L1 might enhance breast cancer proliferation and invasion through the AKT signaling pathway. The method by which BAIAP2L1 modulates the AKT signaling pathway was investigated by MS, which indicated that CAP1 and RPL3 might be involved in the AKT signaling pathway. Subsequent endogenous Co-IP and immunofluorescence assays suggested that BAIAP2L1 interacted and co-localized with RPL3 in the cytoplasm of breast cancer cells. Splicing mutant plasmids were designed by depleting the I-BAR, SH3, and F-actin-binding domains of BAIAP2L1. Co-immunoprecipitation assays were carried out, which indicated that the central SH3 domain of BAIAP2L1 and AA202-288 of RPL3 are responsible for their binding. Wu et al. previously reported that the SH3 domain of BAIAP2L1 is crucial for BAIAP2L1 and SHP2 interaction,[22] but our results did not correlate with these findings. Furthermore, our finding indicated that BAIAP2L1 could activate AKT signaling by stabilizing PIK3CA, a crucial upstream protein of PI3K-AKT signaling, which was dependent on binding with RPL3. The PIK3CA protein was reported to be degraded by ubiquitination,[23–25] and our GSEA and RNA sequencing results also indicated that both BAIAP2L1 and RPL3 might be involved in ubiquitin-mediated proteolysis. Further studies should be carried out to test whether interaction between BAIAP2L1 and RPL3 might stabilize PIK3CA by affecting its ubiquitination, thus promoting the signal transduction of the PI3K-AKT pathway.

Cancer stem cell expansion, induced by EMT and PI3K-AKT signaling, has been reported to promote breast cancer chemotherapy resistance.[26–30] Our results revealed that BAIAP2L1 expression was increased in docetaxel-resistant cells and that BAIAP2L1 expression in breast cancer patients with poor chemotherapy responses,

evaluated by MP grades, was significantly higher than that in patients with better responses.

A recent study by Pipatpanyanugoon et al. reported that BAIAP2L1 might promote cancer cell migration by modulating the phosphorylation of cofilin,[31] which was consistent with our finding that BAIAP2L1 might facilitate cancer cell motility; moreover, it has been proven that AKT signaling could dominate cofilin during cancer progression.[22-34] The AKT–cofilin axis is involved in chemotherapy

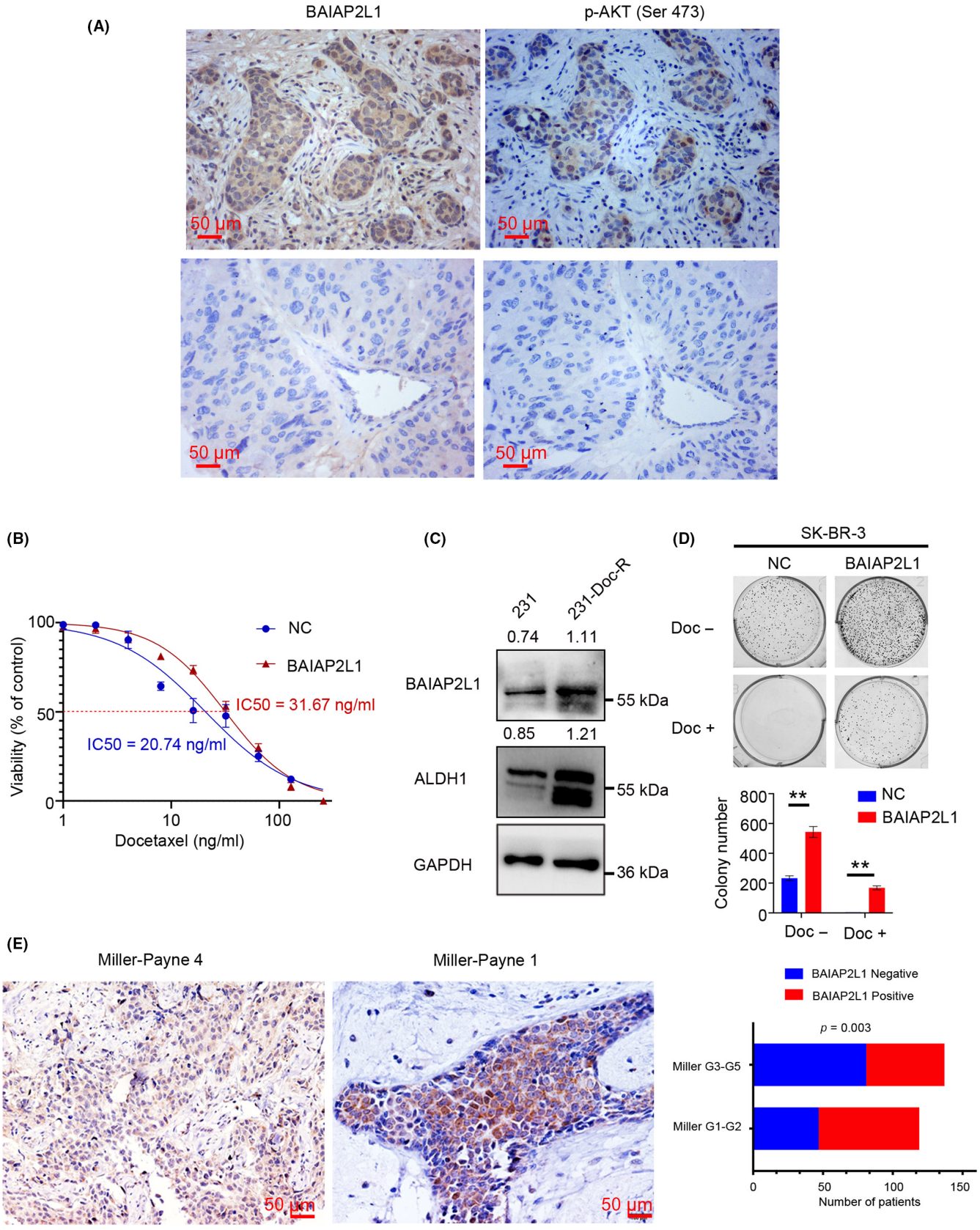

FIGURE 7 BAIAP2L1 promotes chemotherapy resistance of breast cancer cells. (A) Representative images of immunohistochemistry staining of BAIAP2L1 and phosphorylated AKT in Ser473 in patients with breast cancer. Scale bar, 50 μm. (B) IC_{50} values upon BAIAP2L1 overexpression in docetaxel-treated SK-BR-3 cells. (C) Western blot analysis of BAIAP2L1 and cancer stem cell marker aldehyde dehydrogenase 1 (ALDH1) expression in SK-BR-3 docetaxel (Doc)-resistant and parental cells. (D) Colony formation assays were performed to examine the effects on proliferation upon BAIAP2L1 overexpression post docetaxel treatment (E) Representative images of immunohistochemistry staining of BAIAP2L1 in patients with breast cancer within Miller–Payne 3–5 group (responsive group) or 1–2 group (resistant group). Scale bar, 50 μm. Quantification data are expressed as average ± SD of three independent experiments. ** $p < 0.01$, *t*-test, two-sided. NC, Negative control

TABLE 3 Correlation of cytosolic BAIAP2L1 with expression of p-AKT in 59 breast cancer specimens

	BAIAP2L1			
p-AKT	Negative	Positive	*r*	*p* value
Negative	17	8	0.545	<0.001
Positive	5	29		

resistance.[35] Further studies should explore whether cofilin is crucial in the AKT signaling pathway in promoting breast cancer progression.

Our study revealed that BAIAP2L1 was highly expressed in breast cancer, especially in TNBC, and positively correlated with advanced TNM stage, lymph node metastasis, and poor prognosis. Overexpression of BAIAP2L1 was shown to promote breast cancer cell proliferation and invasion in vitro and in vivo by activating the

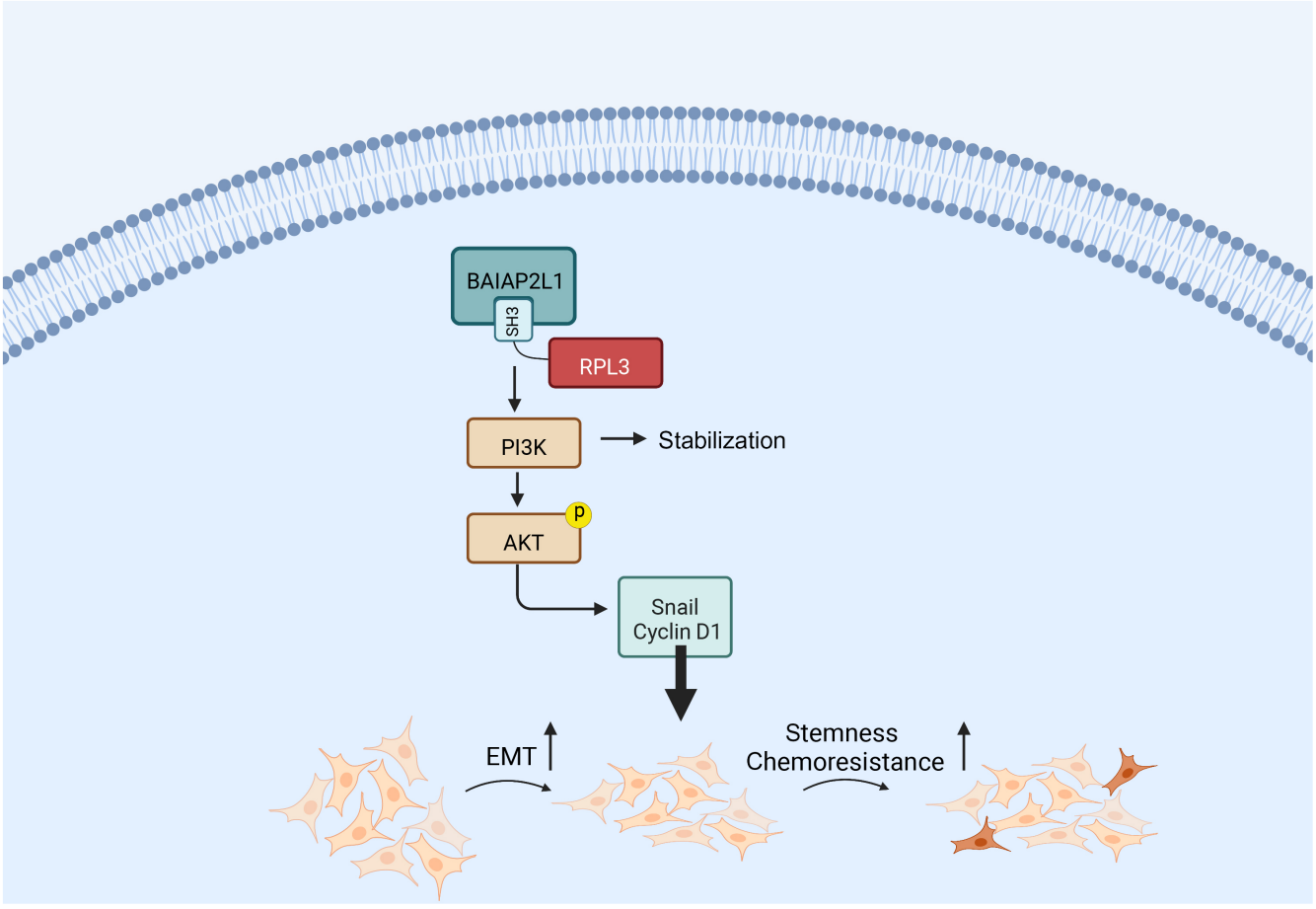

FIGURE 8 Pathway diagram for BAIAP2L1 action in breast cancer cell lines. EMT, epithelial–mesenchymal transition; RPL3, ribosomal protein L3; SH3, SRC homology 3

AKT signaling pathway by stabilizing PIK3CA through binding with RPL3, thus causing chemotherapy resistance.

AUTHOR CONTRIBUTIONS

ND and YZ performed study concept and design. ND and XZ performed development of methodology and writing, review, and revision of the paper. ND, XZ, and YZ provided acquisition, analysis, and interpretation of data, and statistical analysis. YZ provided technical and material support. All authors read and approved the final paper.

ACKNOWLEDGMENTS

None.

FUNDING INFORMATION

This work was supported by the Fundamental Research Funds for Central Universities (LD202121).

CONFLICT OF INTEREST

The authors have no conflict of interest.

ETHICAL APPROVAL

Approval of the research protocol by an institutional review board: The study protocol was approved by the Institutional Review Board of China Medical University.

Informed consent: All participants provided written informed consent, and the study was conducted according to the Declaration of Helsinki principles.

Registry and registration no. of the study/trial: None.

Animal studies: The animals used in this study were treated according to the NIH Guide for the Care and Use of Laboratory Animals (NIH Publications No. 8023, revised 1978).

ORCID

Yong Zhang https://orcid.org/0000-0001-9124-6281

REFERENCES

1. Sung H, Ferlay J, Siegel RL, et al. Global cancer statistics 2020: GLOBOCAN estimates of incidence and mortality worldwide for 36 cancers in 185 countries. *CA Cancer J Clin*. 2021;71(3):209-249.
2. Harbeck N, Gnant M. Breast cancer. *Lancet (London, England)*. 2017;389(10074):1134-1150.
3. Prat A, Pineda E, Adamo B, et al. Clinical implications of the intrinsic molecular subtypes of breast cancer. *Breast*. 2015;24(Suppl 2):S26-S35.
4. Bai X, Ni J, Beretov J, Graham P, Li Y. Cancer stem cell in breast cancer therapeutic resistance. *Cancer Treat Rev*. 2018;69:152-163.
5. Mani SA, Guo W, Liao MJ, et al. The epithelial-mesenchymal transition generates cells with properties of stem cells. *Cell*. 2008;133(4):704-715.
6. Dong C, Yuan T, Wu Y, et al. Loss of FBP1 by snail-mediated repression provides metabolic advantages in basal-like breast cancer. *Cancer Cell*. 2013;23(3):316-331.
7. Pastushenko I, Mauri F, Song Y, et al. Fat1 deletion promotes hybrid EMT state, tumour stemness and metastasis. *Nature*. 2021;589(7842):448-455.
8. Chao A, Tsai CL, Jung SM, et al. BAI1-associated protein 2-like 1 (BAIAP2L1) is a potential biomarker in ovarian cancer. *PLoS One*. 2015;10(7):e0133081.
9. Xu L, Du H, Zhang Q, et al. BAI1-associated protein 2-like 2 is a potential biomarker in lung cancer. *Oncol Rep*. 2019;41(2):1304-1312.
10. Huang LY, Wang X, Cui XF, et al. IRTKS is correlated with progression and survival time of patients with gastric cancer. *Gut*. 2018;67(8):1400-1409.
11. Wang YP, Huang LY, Sun WM, et al. Insulin receptor tyrosine kinase substrate activates EGFR/ERK signalling pathway and promotes cell proliferation of hepatocellular carcinoma. *Cancer Lett*. 2013;337(1):96-106.
12. Ogston KN, Miller ID, Payne S, et al. A new histological grading system to assess response of breast cancers to primary chemotherapy: prognostic significance and survival. *Breast*. 2003;12(5):320-327.
13. Zhang X, Yu X, Jiang G, et al. Cytosolic TMEM88 promotes invasion and metastasis in lung cancer cells by binding DVLS. *Cancer Res*. 2015;75(21):4527-4537.
14. Dong QZ, Wang Y, Tang ZP, et al. Derlin-1 is overexpressed in non-small cell lung cancer and promotes cancer cell invasion via EGFR-ERK-mediated up-regulation of MMP-2 and MMP-9. *Am J Pathol*. 2013;182(3):954-964.
15. Amat S, Penault-Llorca F, Cure H, et al. Scarff-bloom-Richardson (SBR) grading: a pleiotropic marker of chemosensitivity in invasive ductal breast carcinomas treated by neoadjuvant chemotherapy. *Int J Oncol*. 2002;20(4):791-796.
16. Ye X, Tam WL, Shibue T, et al. Distinct EMT programs control normal mammary stem cells and tumour-initiating cells. *Nature*. 2015;525(7568):256-260.
17. Wu Y, Deng J, Rychahou PG, Qiu S, Evers BM, Zhou BP. Stabilization of snail by NF-kappaB is required for inflammation-induced cell migration and invasion. *Cancer Cell*. 2009;15(5):416-428.
18. Hasan R, Zhou GL. The cytoskeletal protein cyclase-associated protein 1 (CAP1) in breast cancer: context-dependent roles in both the invasiveness and proliferation of cancer cells and underlying cell signals. *Int J Mol Sci*. 2019;20(11):2653.
19. Bergqvist M, Elebro K, Sandsveden M, Borgquist S, Rosendahl AH. Effects of tumor-specific CAP1 expression and body constitution on clinical outcomes in patients with early breast cancer. *Breast Cancer Res*. 2020;22(1):67.
20. Hellwig B, Madjar K, Edlund K, et al. Epsin family member 3 and ribosome-related genes are associated with late metastasis in estrogen receptor-positive breast cancer and long-term survival in non-small cell lung cancer using a genome-wide identification and validation strategy. *PLoS One*. 2016;11(12):e0167585.
21. Zhang X, Han J, Feng L, et al. DUOX2 promotes the progression of colorectal cancer cells by regulating the AKT pathway and interacting with RPL3. *Carcinogenesis*. 2021;42(1):105-117.
22. Wu C, Cui X, Huang L, et al. IRTKS promotes insulin signaling transduction through inhibiting SHIP2 phosphatase activity. *Int J Mol Sci*. 2019;20(11):2834.
23. Wang Z, Dang T, Liu T, et al. NEDD4L protein catalyzes ubiquitination of PIK3CA protein and regulates PI3K-AKT signaling. *J Biol Chem*. 2016;291(33):17467-17477.
24. Wang Z, Liu Y, Huang S, Fang M. TRAF6 interacts with and ubiquitinates PIK3CA to enhance PI3K activation. *FEBS Lett*. 2018;592(11):1882-1892.
25. Jiang J, Xu Y, Ren H, et al. MKRN2 inhibits migration and invasion of non-small-cell lung cancer by negatively regulating the PI3K/Akt pathway. *J Exp Clin Cancer Res*. 2018;37(1):189.
26. Butti R, Gunasekaran VP, Kumar TVS, Banerjee P, Kundu GC. Breast cancer stem cells: biology and therapeutic implications. *Int J Biochem Cell Biol*. 2019;107:38-52.

27. Su S, Chen J, Yao H, et al. CD10(+)GPR77(+) cancer-associated fibroblasts promote cancer formation and chemoresistance by sustaining cancer stemness. *Cell*. 2018;172(4):841-856.e816.
28. Jabbarzadeh Kaboli P, Salimian F, Aghapour S, et al. Akt-targeted therapy as a promising strategy to overcome drug resistance in breast cancer - a comprehensive review from chemotherapy to immunotherapy. *Pharmacol Res*. 2020;156:104806.
29. Guerrero-Zotano A, Mayer IA, Arteaga CL. PI3K/AKT/mTOR: role in breast cancer progression, drug resistance, and treatment. *Cancer Metastasis Rev*. 2016;35(4):515-524.
30. Araki K, Miyoshi Y. Mechanism of resistance to endocrine therapy in breast cancer: the important role of PI3K/Akt/mTOR in estrogen receptor-positive, HER2-negative breast cancer. *Breast Cancer*. 2018;25(4):392-401.
31. Pipatpanyanugoon N, Wareesawetsuwan N, Prasopporn S, et al. BAIAP2L1 enables cancer cell migration and facilitates phosphocofilin asymmetry localization in the border cells. *Cancer Comm*. 2022;42(1):75-79.
32. Yao B, Li Y, Chen T, et al. Hypoxia-induced cofilin 1 promotes hepatocellular carcinoma progression by regulating the PLD1/AKT pathway. *Clin Transl Med*. 2021;11(3):e366.
33. Li J, Yang R, Yang H, et al. NCAM regulates the proliferation, apoptosis, autophagy, EMT, and migration of human melanoma cells via the Src/Akt/mTOR/cofilin signaling pathway. *J Cell Biochem*. 2020;121(2):1192-1204.
34. Zhu Y, Xu Y, Chen T, et al. TSG101 promotes the proliferation, migration, and invasion of human glioma cells by regulating the AKT/GSK3β/β-catenin and RhoC/cofilin pathways. *Mol Neurobiol*. 2021;58(5):2118-2132.
35. Sun MY, Xu B, Wu QX, et al. Cisplatin-resistant gastric cancer cells promote the chemoresistance of cisplatin-sensitive cells via the Exosomal RPS3-mediated PI3K-Akt-Cofilin-1 signaling Axis. *Front Cell Dev Biol*. 2021;9:618899.

SUPPORTING INFORMATION

Additional supporting information can be found online in the Supporting Information section at the end of this article.

How to cite this article: Deng N, Zhang X, Zhang Y. BAIAP2L1 accelerates breast cancer progression and chemoresistance by activating AKT signaling through binding with ribosomal protein L3. *Cancer Sci*. 2023;114:764-780. doi:10.1111/cas.15632